Journal of Medical Ultrasound (2011) 19, 81—86

Available online at www.sciencedirect.com

SciVerse ScienceDirect

journal homepage: www.jmu-online.com

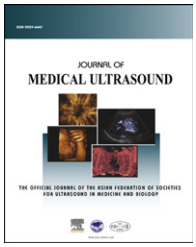

ORIGINAL ARTICLE

Numerical Investigation of Superharmonic Imaging Using Chirp Excitation

Narendra D. Londhe*, R.S. Anand

Indian Institute of Technology Roorkee, Roorkee, India

Received: March 21, 2011; accepted June 15, 2011
Available online October 1, 2011

KEY WORDS
chirp,
harmonic,
imaging,
superharmonic,
ultrasound

At present, along with the fundamental method of ultrasound imaging, tissue harmonic imaging based on imprinting of the second harmonic component is established as the standard method of ultrasound imaging. Recently introduced superharmonic imaging (SHI) has an edge over this standard method and has improved spatial resolution. To explore further advancement in ultrasound imaging for enhanced resolution and penetration depth. SHI is the summation of higher harmonics generated due to nonlinear tissue propagation of ultrasound. Here, the addition of third, fourth and fifth harmonics has been done for the superharmonic field. The modeling of nonlinear wave propagation is done in frequency domain on the basis of the second order operator splitting approach. The higher harmonic components are picked up using the inverse filters. The standard evaluation parameters were significantly improved with linear frequency modulation (FM) chirp. The axial level was 2.8 times higher with linear FM chirp as compared to conventional short pulse. Minor benefits such as a 5% increase in beam width and suppression of side lobes were also recorded. This numerical investigation confirms that linear FM chirp in SHI provides better resolution and penetration depth. State of the art fundamental and second harmonic ultrasound imaging techniques were also improved with linear FM chirp as compared with conventional excitation. SHI is superior to the existing diagnostic ultrasound techniques.

Introduction

Tissue harmonic imaging (THI) is a well-established ultrasound imaging technique in which higher harmonics, specifically the second harmonic, is used to form an

* Correspondence to: Narendra D. Londhe, Department of Electrical Engineering, National Institute of Technology Raipur, G.E. Road, Raipur (C.G.), PIN — 492010, India.
E-mail address: nlondhe.ele@nitrr.ac.in (N.D. Londhe).

0929-6441 © 2011, Elsevier Taiwan LLC and the Chinese Taipei Society of Ultrasound in Medicine. Open access under CC BY-NC-ND license.
doi:10.1016/j.jmu.2011.08.003

ultrasound image [1]. A new imaging technique named superharmonic imaging (SHI) has been proposed recently [2]. It takes an advantage of higher harmonics arises from nonlinear propagation or ultrasound contrast agent response [3]. Moreover, there is better suppression of near-field artifacts, and tissue SHI is expected to improve axial and lateral resolution, resulting in clearer images than with second-harmonic imaging [3,4]. The specialized interleaved array transducer [3,5] has also been designed, which has confirmed the advantages of SHI. However, it has also been reported that it suffers from unwanted harmonic ripples in the frequency band, which generates ghost echoes. This limits the usefulness of SHI with limited penetration and signal-to-noise ratio (SNR). Recently, a dual pulse method [6,7] has been proposed to avoid ghost echoes but it suffers from reduced frame rate and high attenuation. For this, coded excitations can be used, which have been used earlier for second harmonic imaging and have shown improved SNR. Coded excitation using frequency modulated signals (chirps) have previously shown promising results *in vitro* [8] and *in vivo* [9] for fundamental [9] and second harmonic [10] imaging. It has been concluded that linear frequency modulation (FM) chirps significantly improve penetration depth and image quality as well. This surely helps sonographers to resolve diagnostic uncertainty or failed scans due to insufficient penetration, and the use of higher frequency yields higher resolution [11]. Coded excitations have also been reported to have a higher contrast to tissue ratio and SNR for contrast harmonic imaging [12].

In this study, we performed numerical investigation of SHI using chirp excitation. Along the propagation axis, we used numerical algorithms based on frequency domain, the angular spectrum method for calculating diffraction, and solution of Burger's equation for solving nonlinearity of the medium. These are the well-established method but have never been used to investigate SHI that too in modulated version to work with linear FM chirp excitation.

Methods

Linear FM chirp exciting a linear phased array transducer produced an acoustic field that was propagated through the tissue medium. While propagating through the medium, the field suffered from diffraction, absorption and a nonlinear effect due to which the field expanded, attenuated and distorted. This propagation philosophy was resolved using the algorithms shown in Fig. 1. The field was calculated for every small propagation step size increment of Δz. This is also referred to as second order operator splitting. a brief review of the methodologies used for calculating diffraction (angular spectrum method) and nonlinearity and attenuation (frequency domain solution of Burger's equation) is given in the following sections.

Nonlinearity algorithm

Burger's equation

It is convenient to start by considering a theoretical concept, that is, the infinite plane wave travelling in a lossless medium. This makes it possible to ignore the near-field diffractive variations resulting from the finite size of the ultrasound source, and also any changes in pressure amplitude and frequency spectrum resulting from attenuation. An equation that describes nonlinear plane wave propagation in lossless medium in positive z direction can be obtained by discarding the absorption term in Burger's equation. The initial form of a nonlinear Burger's equation is [13]:

$$\frac{\partial p}{\partial z}=\frac{\beta p}{\rho_0 c_0^3}\frac{\partial p}{\partial t'}+\frac{\delta}{2c_0^3}\frac{\partial^2 p}{\partial t'^2} \tag{3}$$

where the retarded time is given by $t=t|z/c_0$. The term on the left of the equation represents propagation and the two terms on the right represent nonlinearity (with the parameter β) and diffusivity (with the parameter δ).

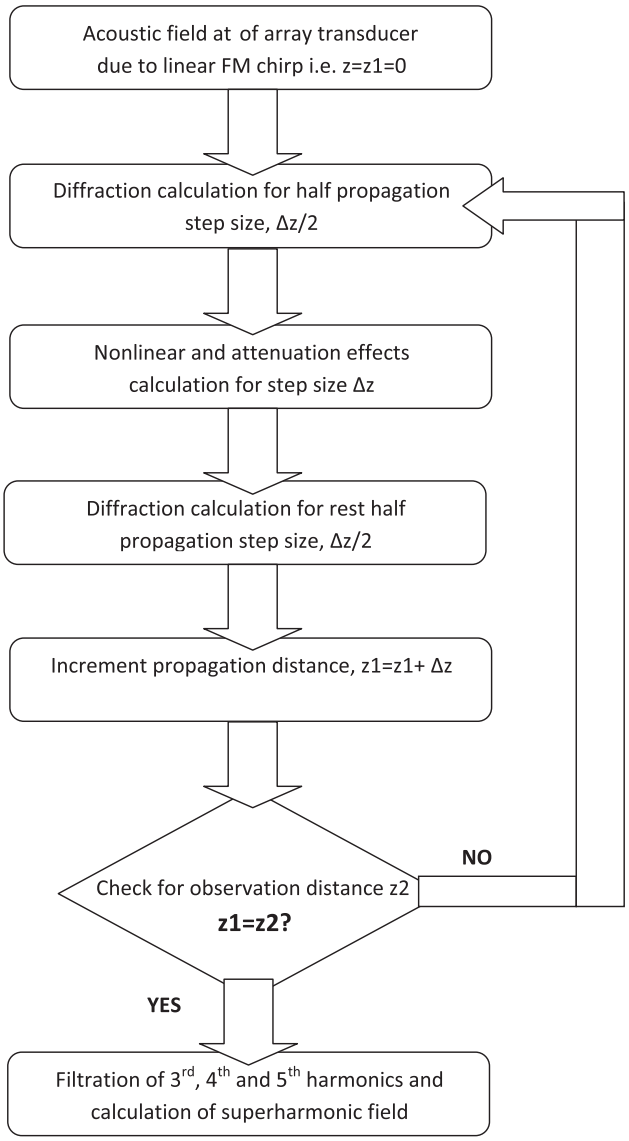

Fig. 1 Flow of numerical calculations proposed in the method (second order operating approach) to measure the superharmonic field at the observation point z2.

This equation can be normalized to represent a dimensionless form, with the following variable substitutions:

$$P=\frac{p}{p_0}, \sigma=\frac{z}{\bar{z}}, \tau=\omega_0 t', A=\alpha_0\bar{z} \tag{4}$$

where the plane wave shock propagation distance is $\bar{z}=\rho_0 c_0^3/\beta p_0\omega_0$, and the absorption coefficient is $\alpha_0=\delta\omega_0^2/2c_0^3$.

$$\frac{\partial P}{\partial\sigma}=P\frac{\partial P}{\partial\tau}+A\frac{\partial^2 P}{\partial^2\tau} \tag{5}$$

According to Cole—Holf transformation, we can transform the Burger's equation to the linear diffusion equation:

$$\frac{\partial P}{\partial\sigma}=\frac{1}{\Gamma}\frac{\partial^2 P}{\partial^2\tau} \tag{6}$$

where Γ is a Goldberg number, which jointly represents the effects of nonlinearity and attenuation.

Frequency domain solution

Burger's equation (6) describes the propagation of nonlinear progressive waves in an absorbing medium. A general solution to the Burgers' equation for a sinusoidal driving pressure, derived by transforming the nonlinear equation into a linear diffusion equation via the Cole—Holf transformation discussed in [14] is given as:

$$\frac{p}{p_0}=\frac{-4}{\Gamma}\frac{\sum_{n=1}^{\infty} n(-1)^n I_n(\Gamma/2)\exp\left(-n^2\sigma/\Gamma\right)\sin n\omega_0 t'}{I_0(\Gamma/2)+2\sum_{n=1}^{\infty} n(-1)^n I_n(\Gamma/2)\exp(-n^2\sigma/\Gamma)\cos n\omega_0 t'} \tag{7}$$

where I_n is the modified Bessel function of the first kind of order n, and $\Gamma=1/\alpha_0\bar{z}$ is the Goldberg number that indicates the ratio of nonlinearity to absorption of the medium. This solution converges very slowly when $\Gamma >> 1$ (strong nonlinear medium), so the following Fay's equation can be used for $\Gamma >> 1$ and $\sigma > 3$:

$$\frac{p}{p_0}=\frac{2}{\Gamma}\sum_{n=1}^{\infty}\frac{\sin n\omega_0 t'}{\sinh[n(1+\sigma)/\Gamma]} \tag{8}$$

Diffraction algorithm

It is sufficient to mention that, for each frequency component of the source excitation, there exists a spatial frequency representation of the source plane.[10,11] Propagation from one plane to another may be accomplished through use of a transfer function H.

Angular spectrum method

Let us assume that the surface velocity of the source plane is $v(x, y, z_o, t)$. First, we need to perform a FFT (Fast Fourier Transform) in order to find the frequency domain representation of the velocity $s(x, y, z_o, \omega)$ for each point (x, y) in the source plane. Once $s(x, y, z_o, \omega)$ is found for all points (x, y) in the transducer plane, and for all frequency components ω, the following steps are needed: [15,16]

For each frequency component ω, (1) perform a 2D-FFT on $s(x, y, z_o, \omega)$ to obtain $S(k_x, k_y; z = z_o)$; (2) multiply S by the transfer function $H(k_x, k_y; z_o|z_1)$ as given below; and (3)

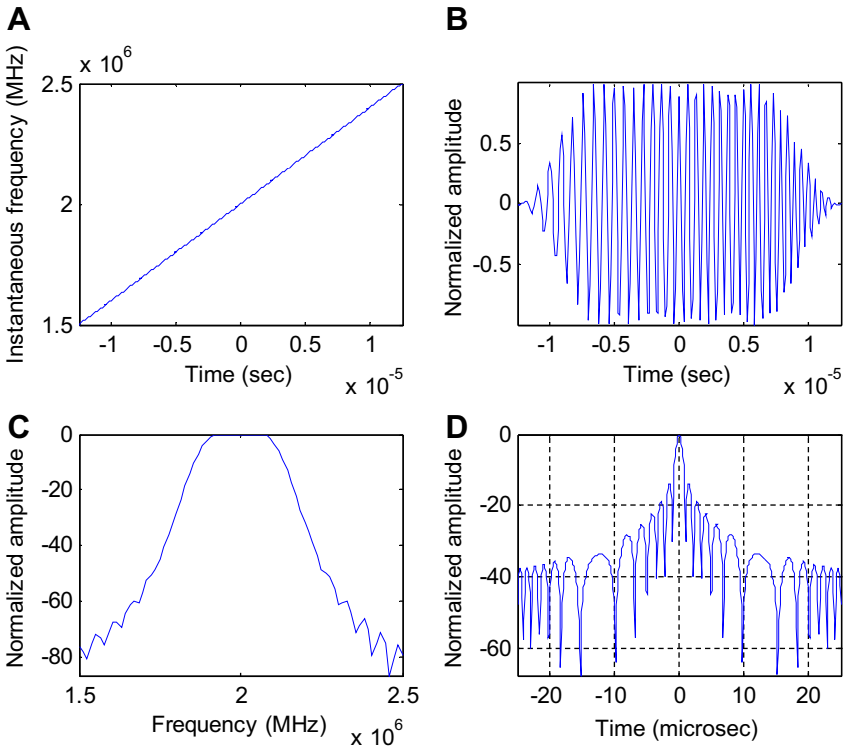

Fig. 2 (A) Instantaneous frequency versus time; (B) Linear frequency modulation chirp waveform; (C) its frequency spectrum; (D) time autocorrelation function, obtained with center frequency 2 MHz, bandwidth 1 MHz, and pulse duration 25 microseconds.

perform a IFFT (Inverse Fast Fourier Transform) to obtain the frequency domain velocity s(x, y, z_1, ω).

Finally, once s(x, y, z_1, ω) has been computed for all points (x, y) on the plane $z = z_1$, and for all frequencies ω, do an IFFT on s(x, y, z_1, ω), enabling the time domain velocity waveform v(x, y, z_1, t) to be obtained. This should be done for all points (x, y) in the plane $z = z_1$. The angular spectrum method is computationally efficient compared to the Rayleigh and impulse response methods, given a nonuniform, nonaxisymmetric surface velocity on the transducer/source plane.

$$H(k_x, k_y : \Delta z) = \begin{cases} e^{j\Delta z\sqrt{k^2-(k_x^2+k_y^2)}} \text{ for } \left(k_x^2+k_y^2\right) \le k^2 \\ e^{-\Delta z\sqrt{k_x^2+k_y^2-k^2}} \text{ for } \left(k_x^2+k_y^2\right) > k^2 \end{cases} \quad (9)$$

The purpose of the transfer function is to assign a phase that needs to realize the Huygen's principle; according to which, the wave components are added linearly as per their phase relationships.

Linear FM excitation (chirp)

Pulse compression comprised of all the pulses with some kind of frequency modulation and its simplest form is a linear frequency modulation (LFM) signal. A unit amplitude frequency-modulated pulse with linear variation of instantaneous frequency f_i , with time t, is expressed as:

$$f_i = f_c + \frac{B}{T}t, \ldots \frac{-T}{2} \le t \le \frac{T}{2} \quad (10)$$

where f_c is the center frequency, B is the pulse bandwidth, and T is the pulse duration. The parameter B/T is often denoted as μ, and referred to as the FM slope or the rate of FM sweep. The pulse sweeps linearly the frequencies in the interval $f_c - B/2$ to $f_c + B/2$. The linear FM pulse with center frequency, f_c expressed as:

$$\zeta(t) = w_t(t)\cdot\exp\left[j2\pi\left(\left(f_c+\frac{B}{2}\right)t+\frac{B}{2T}t^2\right)\right] \quad (11)$$

where $w_t(t)$ is weight function. In our work, a Tukey window is used as the weight function. The linear FM pulse shown in Fig. 2 used in the simulations, and its frequency spectrum and time autocorrelation are also shown.

Results

Linear phased array imaging using linear FM chirp

Here, we considered a linear phased array with no beam-steering, no apodization, and no lens in the elevation plane. The array considered had 64 elements of width $\lambda/2$, and spaced $\lambda/4$ apart, where the operating frequency was 2 MHz. Elements were of height 1 cm, and the array was phased such that the focal distance was 10 cm. The length of the transducer was 3.7 cm, and the continuous wave excitation was of amplitude 500 kPa. Propagation was in a soft tissue medium with $\beta = 5$ and $\alpha = 0.3$ dB/cm at 1 MHz.

Fig. 3A shows the linear FM signature used for exciting a circular ultrasound transducer for imaging. The axial

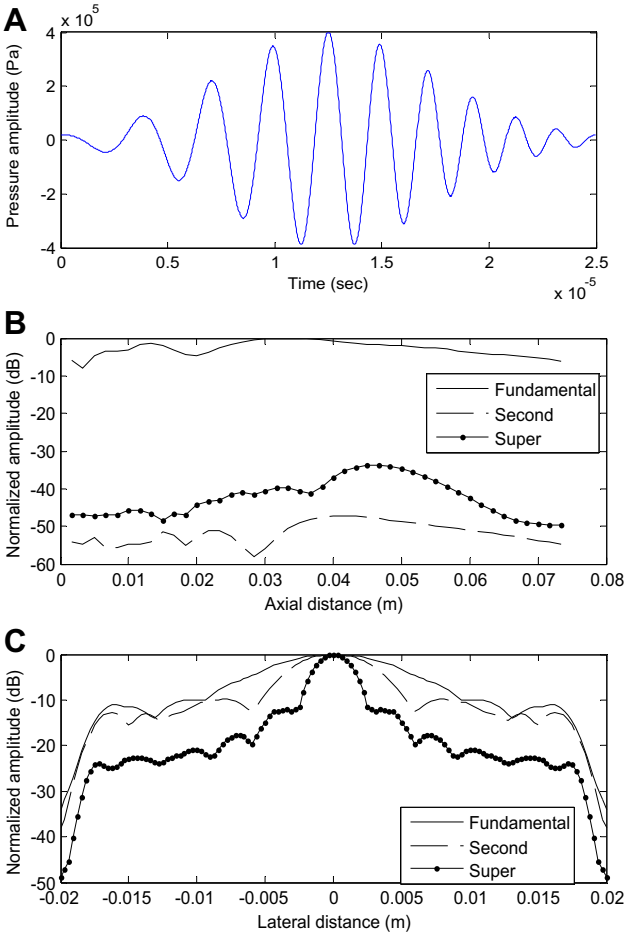

Fig. 3 (A) Linear frequency modulation (chirp) signal of center frequency, fc = 2.0 MHz and bandwidth = 0.5. (B) Axial spectral profiles and (C) lateral spectral profiles at z = 35 mm of fundamental (solid), second harmonic (dashed) and superharmonic (dotted) frequency components.

spectral profiles of fundamental, second harmonic and superharmonic are shown in Fig. 3B. The second harmonic energy is 40 dB below fundamental energy, whereas superharmonic energy is 33 dB below the fundamental energy at the surface of the transducer. The superharmonic component builds rapidly along the transmission distance and also becomes maximal at the focal point. After the focal point, it remains close to the second harmonic and by the end of the propagation distance, the superharmonic remains 43 dB below the fundamental energy while the second harmonic is 48 dB below. Therefore, SHI with linear FM excitation energy is promising at imaging distances.

Fig. 3C shows the lateral spectral profiles of fundamental, second harmonic and superharmonic frequency components. From Fig. 3C, the beam width of the superharmonic is 3.75 mm, and 8.12 mm and 14.37 mm for the second harmonic and fundamental components. This clearly indicates that, with linear FM excitation, the lateral resolution for SHI is far better than second harmonic and fundamental imaging. Moreover, deposition of superharmonic energy is greater in the central part of the beam, therefore, adequate reduction in side lobes is observed. The superharmonic energy available for scattering is 12.54 dB

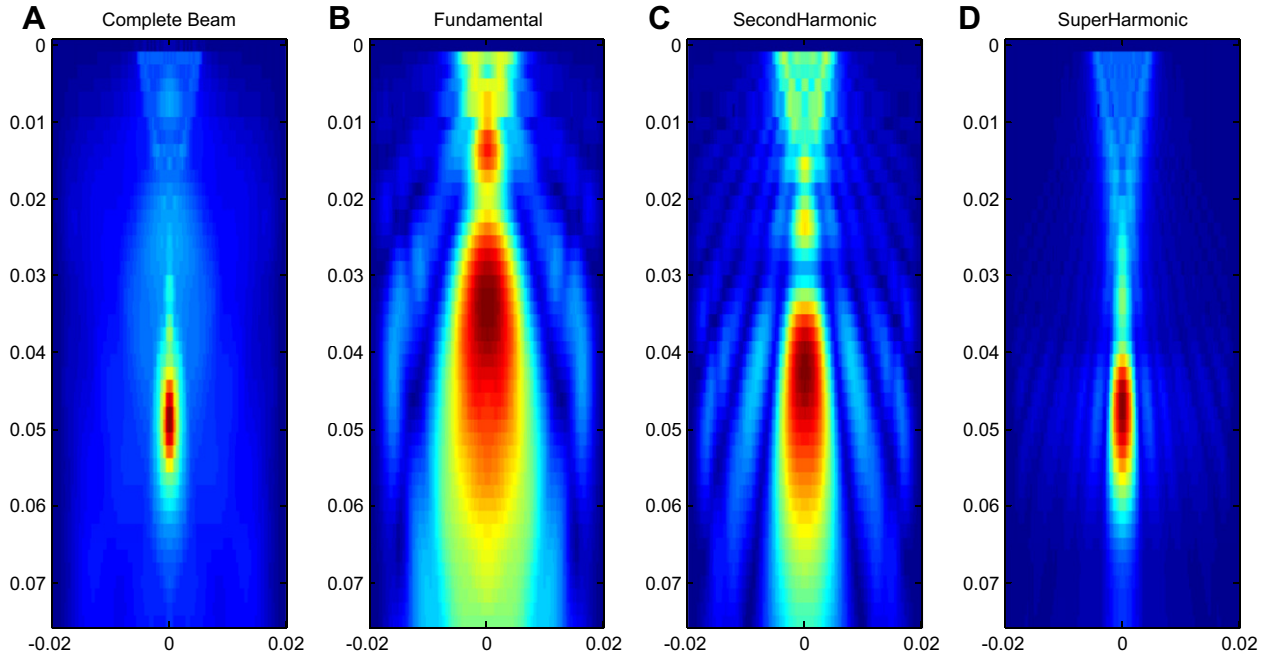

Fig. 4 Azimuthal spectral profiles for a 2-MHz circular transducer of radius 10 mm and focus of 50 mm in both azimuthal and elevation directions. (A) Complete beam spectral profile; (B) fundamental spectral profile; (C) second harmonic spectral profile; and (D) superharmonic spectral profile.

below the fundamental energy, while second harmonic energy has higher scattering energy available at 10.14 dB below fundamental energy. The scattering from the objects located at the edges of the beam is less in SHI compared to second harmonic imaging (THI). In the elevation plane, even when no lens is used, the superharmonic profile is narrower. In phased array B-mode imaging, fundamental side lobes are known to be particularly troublesome, causing clutter artifacts. For superharmonic side lobes, however, it seems that attenuation dominates over nonlinearity, and thus clutter artifacts may be reduced by using the superharmonic signal. Fig. 4A shows complete field distribution and Figs. 4B–D shows the fundamental, second harmonic and superharmonic field distributions of the transducer over a plane defined by the axial and lateral coordinate axes.

SHI and THI takes the benefit of the nonlinear wave propagation of ultrasound waves in tissue and the associated generation of higher harmonics to obtain potentially improved resolution images. However, the higher harmonics are weaker than the fundamental component, therefore, it may be beneficial to use coded excitations to improve SNR and penetration depth. There are significant observations here as per the results mentioned in the above section pertaining to propagation of conventional and linear FM pulses, such as behavioral study of second harmonic and superharmonic components and notification of improvement in resolution, SNR and penetration depth. The results are summarized in Table 1, where SHI has been investigated with linear FM chirp and compared with their existing counterparts' fundamental and THI.

The superharmonic frequency component of the distorted ultrasound wave provides substantial improvement in resolution. This has also been reported previously by other researchers. However, with coded excitation, the resolution has improved further. The beam width of the superharmonic lateral beam profile is reduced minutely with linear FM pulse (Fig. 4C) as compared to conventional short pulse.

On the same line, THI has also shown significant improvement in lateral resolution with linear FM excitation. For conventional THI, lower and narrower bandwidths are selected for both transmission and reception to avoid overlapping with the fundamental and second harmonic but with the use of wide band transmit and receive band filter for superharmonic imaging ultimately leads to the improved axial resolution.

Table 1 Performance comparison of superharmonic, second harmonic and fundamental acoustic fields.

Excitation	Imaging	Axial level (dB)	Beam width (mm)	Peak side lobe level PSL (dB)
Conventional short pulse	Fundamental	−1.12	6.87	−11.26
	Second harmonic	−32.09	8.12	−10.11
	Superharmonic	**−12.10**	**3.75**	**−12.45**
Linear FM pulse	Fundamental	−2.08	14.37	−10.31
	Second harmonic	−52.11	8.08	−10.14
	Superharmonic	**−34.05**	**3.55**	**−12.54**

The superharmonic component with two types of excitation enters the body with lower energy levels. This may avoid the image artifacts because of reverberations at the boundaries of the body. The linear summation of higher harmonics enhances the energy levels of the superharmonic component as compared to the second harmonic, accordingly improves the SNR with excitations, conventional and linear FM (Fig. 3B and 3C).

Discussion

To date, low SNR and penetration depth have been major concerns for researchers, and as a result, ultrasound imaging has lagged behind other imaging modalities. From the above results and discussion, it can be concluded that coded excitations, linear as well as nonlinear FM, enhance resolution, SNR and penetration depth.

In particular, nonlinear FM pulses enhance SNR as well as resolution for superharmonic imaging by a factor of 3, and they can also penetrate deeper to investigate the critical human organs and their function. The significant improvement in resolution may bring ultrasound imaging into line with high-resolution imaging techniques such as MRI. In conclusion, the coded SHI (CSHI) can be considered as the improved form of SHI as well as THI. The improvements in THI with linear FM pulses i.e. coded THI (CTHI) are also considerable, thus, existing probes for THI can be used for CTHI with minor technical and processing modifications. Rigorous experimental studies are needed to evaluate CTHI and CSHI. Further studies can be done on signal processing and optimized selection of instantaneous frequency pattern in nonlinear CTHI and CSHI, and other work towards coding of excitation may be possible.

References

[1] Bradley C. Mechanisms of image quality improvement in tissue harmonic imaging. AIP 2006;838:247—54.
[2] Bouakaz Jong ND. Native tissue imaging at superharmonic frequencies. IEEE Trans Ultrason Ferroelectr Freq Control 2003;44:125—39.
[3] van Neer PLMJ, Danilouchkine MG, Matte GM, et al. Superharmonic imaging: development of an interleaved phased-array transducer. IEEE Trans Ultrason Ferroelectr Freq Control 2010;57:455—68.
[4] Ma Q, Zhang D, Gong X, et al. Investigation of superharmonic sound propagation and in biological tissues in vitro. J Acoust Soc Am 2006;119:2518—23.
[5] Bouakaz A, Ten Cate AFJ, Jong ND. A new ultrasonic transducer for improved contrast nonlinear imaging. Phys Med Biol 2004;49:3515—25.
[6] Matte G, van Neer PLMJ, Borsboom JMG, et al. A new frequency compounding technique for super harmonic imaging. IEEE Ultrason Symp; 2008:357—60.
[7] van Neer PLMJ, Danilouchkine MG, Matte GM, et al. Dual pulse frequency compounded super harmonic imaging for phased array transducers. IEEE Ultrason Symp; 2009:381—4.
[8] Misaridis TX, Pedersen MH, Jensen JA. Clinical use and evaluation of coded excitation in B-mode images. IEEE Ultrason Symp; 2000:1689—93.
[9] PedersenMH MisaridisTX. JensenJA. Clinical evaluation of chirp-coded excitation in medical ultrasound. Ultrasound Med Biol 2003;29:895—905.
[10] Song J, Kim S, Sohn HY, et al. Coded excitation for ultrasound tissue harmonic imaging. Ultrasonics 2010;50:613—9.
[11] Tranquart F, Grenier N, Eder V, et al. Clinical use of ultrasound tissue harmonic imaging. Ultrasound Med Biol 1999;25: 889—94.
[12] Jerome MG, Borsboom Chin CT, et al. Harmonic chirp imaging method for ultrasound contrast agent. IEEE Trans Ultrason Ferroelectr Freq Control 2005;52:241—9.
[13] Duck FA. Nonlinear acoustics in diagnostic ultrasound. Ultrasound Med Biol 2002;28:1—18.
[14] Blackstock DT. Connection between the Fay and Fubini solutions for plane sound waves of finite amplitudes. J Acoust Soc Am 1966;39:1019—26.
[15] Belgroune D, Belleval DJF, Djelouah H. Modelling of the ultrasonic field by the angular spectrum method in presence of interface. Ultrasonics 2002;40:297—302.
[16] Zemp RJ. Modeling of nonlinear ultrasound propagation in tissue from array transducers. J Acoust Soc Am 2003;113: 139—52.